Astrophysical Masers:
Unlocking the Mysteries of the Universe
Proceedings IAU Symposium No. 336, 2017
A. Tarchi, M.J. Reid & P. Castangia, eds.

doi:10.1017/S1743921317010250

The extraordinary outburst in NGC6334I-MM1: the rise of dust and emergence of 6.7 GHz methanol masers

Todd R. Hunter[1], Crystal L. Brogan[1], James O. Chibueze[2], Claudia J. Cyganowski[3], Tomoya Hirota[4] and Gordon C. MacLeod[5]

[1]National Radio Astronomy Observatory,
520 Edgemont Rd, Charlottesville, VA 22903, USA
email: thunter@nrao.edu

[2]SKA South Africa,
3rd Floor, The Park, Park Road, Pinelands, Cape Town, 7405, South Africa

[3]SUPA, School of Physics and Astronomy, University of St. Andrews,
North Haugh, St. Andrews KY16 9SS, UK

[4]Mizusawa VLBI Observatory, National Astronomical Observatory of Japan,
Osawa 2-21-1, Mitaka-shi, Tokyo 181-8588, Japan

[5]Hartebeesthoek Radio Astronomy Observatory,
PO Box 443, Krugersdorp 1740, South Africa

Abstract. Our 2015-2016 ALMA 1.3 to 0.87 mm observations (resolution $\sim$ 200 au) of the massive protocluster NGC6334I revealed that an extraordinary outburst had occurred in the dominant millimeter dust core MM1 (luminosity increase of 70×) when compared with earlier SMA data. The outburst was accompanied by the flaring of ten maser transitions of three species. We present new results from our recent JVLA observations of Class II 6.7 GHz methanol masers and 6 GHz excited OH masers in this region. Class II masers had not previously been detected toward MM1 in any interferometric observations recorded over the past 30 years that targeted the bright masers toward other members of the protocluster (MM2 and MM3=NGC6334F). Methanol masers now appear both toward and adjacent to MM1 with the strongest spots located in a dust cavity $\sim$1 arcsec (1300 au) north of the MM1B hypercompact HII region. In addition, new excited OH masers appear on the non-thermal source CM2. These data reveal the dramatic effects of episodic accretion onto a deeply-embedded high mass protostar and demonstrate its ongoing impact on the surrounding protocluster.

Keywords. Massive protostars, accretion, masers

1. Introduction

Episodic accretion in protostars is increasingly recognized as being an essential phenomenon in star formation (Evans *et al.* 2009). Outbursts from deeply-embedded low-mass protostars have recently been detected via large increases in their mid-infrared or submillimeter emission, including a Class 0 source HOPS-383 (Safron *et al.* 2015) and a Class I source EC53 (Yoo *et al.* 2017). It has also become clear that massive protostars also exhibit outbursts as evidenced by the 4000 $L_\odot$ erratic variable V723 Carinae (Tapia *et al.* 2015), the far-infrared flare from the 20 $M_\odot$ protostar powering S255IR-NIRS3 (Caratti o Garatti *et al.* 2016), and the ongoing (sub)millimeter flare of the deeply-embedded source MM1 in the massive protocluster NGC6334I (Hunter *et al.* 2017). The large increases in bolometric luminosity observed in these events provide evidence for accretion outbursts similar to those predicted by hydrodynamic simulations of massive star

formation (Meyer *et al.* 2017). Identifying additional phenomena associated with these events will help explore the mechanism of the outbursts, particularly if spectral line tracers can be identified, as they can potentially trace gas motions at high angular resolution. As the brightest line emission emerging from regions of massive star formation, masers offer an important avenue of study, especially since the recent methanol maser flare in S255IR (Moscadelli *et al.* 2017) and the multi-species flares in NGC6334I-MM1 (Brogan *et al.* 2018; MacLeod *et al.* 2018) have provided a direct link between protostellar accretion outbursts and maser flares.

2. Observations

Observations of the massive protocluster NGC6334I were performed with the Karl G. Jansky Very Large Array (VLA)† in A-configuration in Oct.-Nov. 2016 (mean epoch 2016.9). In addition to the coarse resolution spectral windows used to image the continuum emission in C-band (4-8 GHz), we observed several maser transitions with the 8-bit digitizers and high spectral resolution, dual-polarization correlator windows. The 6.66852 GHz (hereafter 6.7 GHz) CH_3OH 5(1)-6(0) A+ line (E_{Lower}=49 K) was observed with a channel spacing of 1.953125 kHz (0.0878 km s^{-1}) over a span of 90 km s^{-1} centered at -7 km s^{-1}. Three lines of excited-state OH maser emission were also observed: J=1/2-1/2, F=0-1 at 4.66024 GHz (E_{Lower}=182 K), and J=5/2-5/2, F=2-2 at 6.03075 GHz and F=3-3 at 6.03509 GHz (both having E_{Lower}=120 K). The data were calibrated using the VLA pipeline with some additional flagging required. The calibrated data were Hanning smoothed to reduce ringing from strong spectral features and then iteratively self-calibrated using the bright continuum emission as the initial model. Multi-scale clean was used with scales of 0, 5, and 15 times the image pixel size to produce Stokes I continuum images with a beamsize of $0.63'' \times 0.14''$. The bright UCHII region (MM3 = NGC 6334F, Hunter *et al.* 2006) limits the dynamic range of the continuum images. Stokes I cubes of the maser emission were made with a channel spacing (and effective spectral resolution) of 0.15 km s^{-1}. We also made cubes of right and left circular polarization for the strongly-polarized high frequency OH lines. The 4.66 GHz OH line was undetected at an rms of 3.3 mJy beam^{-1}.

3. Results

We fit each channel of the maser cubes that had significant emission with an appropriate number of Gaussian sources, using the pixel position of each emission peak and the beam shape as the initial guesses for the fitted parameters. Their positions and relative intensities are shown in Fig. 1. Many maser features have now appeared within the continuum source MM1 and along its eastern and northern peripheries. These are the first detections of Class II methanol maser emission toward this location in nearly 30 years of interferometric observations, all of which were sufficiently sensitive to detect masers of this strength. Previous epochs at 6.7 GHz include Jan. 1992 (Norris *et al.* 1993), May 1992 (Ellingsen *et al.* 1996), July 1994 (Walsh *et al.* 1998), July 1995 (Caswell *et al.* 1997), Sep. 1999 (Dodson *et al.* 2012), Mar. 2005 (Krishnan *et al.* 2013), May 2011 (Brogan *et al.* 2016), and Aug. 2011 (Green *et al.* 2015). In all previous epochs, masers originate only from the UCHII region (NGC6334F) and MM2. In addition, the original VLBI imaging of the Class II 12.2 GHz methanol maser did not detect any features toward

† The National Radio Astronomy Observatory is a facility of the National Science Foundation operated under agreement by the Associated Universities, Inc.

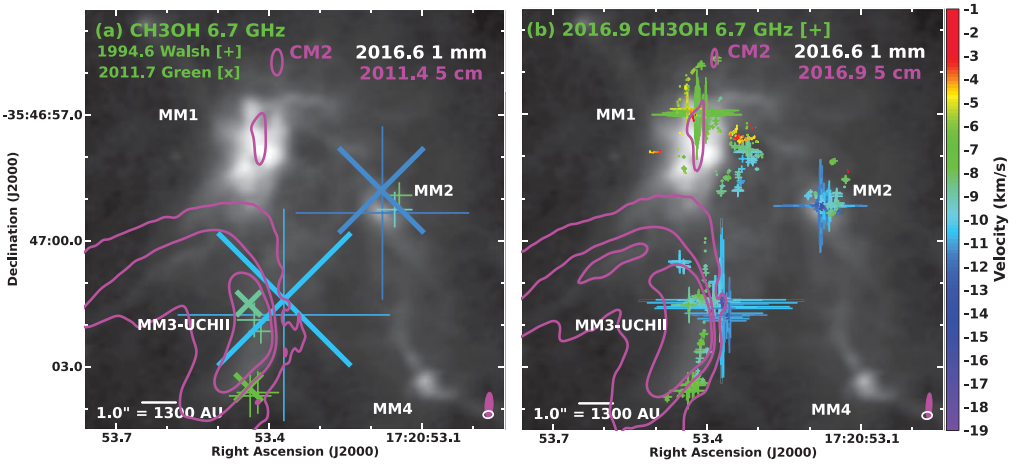

Figure 1. (a) The methanol maser positions (+ symbols) observed by the Australia Telescope Compact Array (ATCA) on July 31, 1994 (Walsh *et al.* 1998) and September 2, 2011 (Green *et al.* 2015) are overlaid on an epoch 2016.6 ALMA 1 mm continuum image in greyscale (Hunter *et al.* 2017). Epoch 2011.5 VLA 5 cm continuum contours are also overlaid with levels of $2.2 \times 10^{-2} \times (4, 260, 600)$ mJy beam^{-1} (Brogan *et al.* 2016). Maser intensity is indicated by the symbol diameter (proportional to the square root of the intensity). The millimeter continuum sources are labeled for reference. (b) Same as (a) but the VLA epoch 2016.9 masers are overlaid.

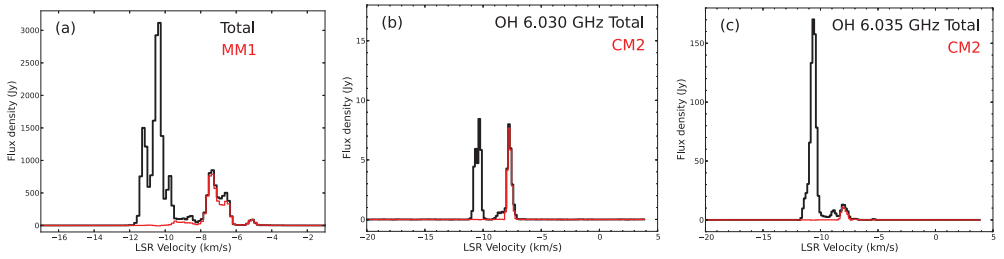

Figure 2. (Panel a) Integrated spectra from the epoch 2016.9 6.7 GHz methanol maser cube taken over all the maser features (upper profile) and from an elliptical region surrounding only the maser features associated with MM1 (lower profile). (Panels b-c) Integrated spectra of the excited-state OH masers constructed by summing the flux from all directions showing emission (upper profiles) and from CM2 only (lower profiles): (b) 6.030 GHz line; (c) 6.035 GHz line.

MM1 (Norris *et al.* 1988), nor are any features toward MM1 reported in the two epochs of the Methanol MultiBeam survey of 12.2 GHz masers (Breen *et al.* 2012).

The brightest features in MM1 (peak = 545 Jy at -7.25 km s^{-1}) lie in the valley of emission in the northern part, between the 1.3 mm continuum sources MM1F and MM1G. This velocity matches that of the thermal hot core emission (-7.3 km s^{-1}, Zernickel *et al.* 2012). The integrated spectrum of MM1 compared to the total field (Figure 2) further demonstrates that the dominant emission arises from -6 to -8 km s^{-1}. Additional strong features appear on MM1F and weaker features near the LSR velocity extend northward from MM1F, with the northernmost spot coincident with the non-thermal radio source CM2. Weak redshifted features lie just south of MM1F. Another set of near-LSR features coincide with the millimeter source MM1C, however the three brightest and most central millimeter sources (MM1A, 1B, and 1D) are notably lacking in any maser emission. A large number of moderate strength, primarily blueshifted masers lie in the cavities of dust

emission located west and southwest of MM1A. Finally, a number of weak, moderately redshifted features lie in the depression between MM1C and MM1E.

The tendency of the new masers to lie along the heated surfaces of dust cavities while avoiding the regions of highest density are consistent with pumping schemes for 6.7 GHz masers. This transition is radiatively pumped by mid-infrared photons (Sobolev & Deguchi 1994), requiring dust temperatures above ∼120 K and gas densities below about 10^8 cm^{-3} (Cragg *et al.* 2005). Following the millimeter continuum outburst, the dust temperature of MM1 exceeds 250 K toward the central components, and was above 150 K over a several square arcsec region (Brogan *et al.* 2016). Prior to the outburst, when the dust and gas temperatures were presumably in better equilibrium, the most compact organic species exhibited excitation temperatures of 100 K (CH_3OH) to 150 K (CH_3CN) (Zernickel *et al.* 2012). Thus, the rapid heating of dust grains by more than ∼100 K by the recent accretion outburst can plausibly explain the appearance of 6.7 GHz masers in the gas in the vicinity of the powering source MM1B. Furthermore, the group of masers to the west and southwest of MM1 coincide with an area of warm dense gas where methanol is abundant, as traced by the 279.3519 GHz thermal transition (E_{lower} = 177 K) in our post-outburst ALMA observations.

In the 6 GHz OH masers, our analysis of Zeeman pairs confirms the north/south dichotomy in the sign of the line-of-sight magnetic field across the UCHII region previously reported by Caswell *et al.* (2011). As shown in Fig. 2b-c, we find a new velocity component at -7 to -8 km s^{-1} that originates from the non-thermal radio continuum source CM2 (Brogan *et al.* 2016). It shows an abnormally comparable intensity ratio between the 6.035 and 6.030 GHz lines and has likely been excited by the recent outburst in MM1 and shows a smaller magnetic field (+0.5 to +3.7 mG) compared to the UCHII region.

References

Breen, S. L., Ellingsen, S. P., Caswell, J. L., *et al.* 2012, *MNRAS* 421, 1703
Brogan, C. L., Hunter, T. R., *et al.* 2018, these proceedings
Brogan, C. L., Hunter, T. R., Cyganowski, C. J., *et al.* 2016, *ApJ* 832, 187
Caratti o Garatti, A., Stecklum, B., Garcia Lopez, R., *et al.* 2016, *Nature* (Physics) 13, 276
Caswell, J. L., Kramer, B. H., & Reynolds, J. E. 2011, *MNRAS* 414, 1914
Caswell, J. L. 1997, *MNRAS* 289, 203
Cragg, D. M., Sobolev, A. M., & Godfrey, P. D. 2005, *MNRAS* 360, 533
Dodson, R. & Moriarty, C. D. 2012, *MNRAS* 421, 2395
Ellingsen, S. 1996, Ph.D. Thesis, University of Tasmania
Evans, N. J., II, Dunham, M. M., Jørgensen, J. K., *et al.* 2009, *ApJ* (Supplement) 181, 321-350
Green, J. A., Caswell, J. L., & McClure-Griffiths, N. M. 2015, *MNRAS* 451, 74
Hunter, T. R., Brogan, C. L., MacLeod, G., *et al.* 2017, *ApJ* (Letters) 837, L29
Hunter, T. R., Brogan, C. L., Megeath, *et al.*, 2006, *ApJ* 649, 888
Krishnan, V., Ellingsen, S. P., Voronkov, M. A., & Breen, S. L. 2013, *MNRAS* 433, 3346
MacLeod, G., *et al.*, 2018, these proceedings
Meyer, D. M.-A., Vorobyov, E. I., Kuiper, R., & Kley, W. 2017, *MNRAS* 464, L90
Moscadelli, L., Sanna, A., Goddi, C., *et al.* 2017, *A&A* 600, L8
Norris, R. P., Caswell, J. L., Wellington, K. J., *et al.* 1988, *Nature* 335, 149
Norris, R. P., Whiteoak, J. B., Caswell, J. L., *et al.* 1993, *ApJ* 412, 222
Safron, E. J., Fischer, W. J., Megeath, S. T., *et al.* 2015, *ApJ* (Letters) 800, L5
Sobolev, A. M. & Deguchi, S. 1994, *A&A* 291, 569
Tapia, M., Roth, M., & Persi, P. 2015, *MNRAS* 446, 4088
Walsh, A. J., Burton, M. G., Hyland, A. R., & Robinson, G. 1998, *MNRAS* 301, 640
Yoo, H., Lee, J.-E., Mairs, S., *et al.* 2017, *ApJ* 849, 69
Zernickel, A., Schilke, P., Schmiedeke, A., *et al.* 2012, *A&A* 546, A87